

β -Nucleators and β -Crystalline Form of Isotactic Polypropylene

MEI-RONG HUANG,¹ XIN-GUI LI,^{1,*} and BO-RONG FANG²

¹Department of Textile Chemistry, Tianjin Institute of Textile Science and Technology, Tianjin 300160, People's Republic of China; ²Department of Chemical Fiber Technology, China Textile University, Shanghai 200051, People's Republic of China

SYNOPSIS

Different levels of β -form crystallinity in isotactic polypropylene (iPP) were produced by blending a series of additives. X-ray diffraction analyses showed that the Kx values varied from 0 to 0.95. Indigosol Brown IRRD, Indigosol Red Violet IRH, Cibantine Orange HR, Indigosol Pink IR, Cibantine Blue 2B, Indigosol Golden Yellow IGK, and Indigosol Grey IBL were found to be effective β -nucleators. The respective Kx values of the iPP samples containing the above seven β -nucleators of 0.05 wt % are 0.54, 0.68, 0.82, 0.82, 0.86, 0.92, and 0.95. All the β -nucleators possess fused benzene rings or heterocycles in their molecular structures. X-ray diffraction studies on them revealed a mutual character in that the strongest or the second-strongest reflections almost locate at the d -spacing of 2.83 Å. The magnitude is about half of that of the β -form crystallinity d -spacing (5.64 Å). The β -form level also depends on a number of factors under our control, such as the β -nucleator concentration, cooling rate, crystallization temperature, and melt temperature. Polarizing microscope observations suggested that β -spherulites possess a bright color and that their Maltese Crosses display some concentric banding of a rather spiky, jagged character. Their lamellae exhibit a correlated and dendritic structure seen by a scanning electron microscope. © 1995 John Wiley & Sons, Inc.

INTRODUCTION

Polymorphism is a well-known effect in crystalline isotactic polypropylene (iPP). There are α , β , γ , and δ crystalline forms involved in the modification of iPP. Of all these crystalline forms, the β -form demonstrates the higher performance, such as higher values of elongation at break and higher impact strength.¹⁻³ In addition, the β -form iPP is a better electret than is the α -form. What is more important is that the β -form would convert into the α -form,^{4,5} consequently resulting in the formation of pinholes when the β -form iPP experiences an extension or heating treatment, owing to the lower density of the β -form than that of the α -form. We can take advantage of this transformation to produce a porous film which can be mimeographed directly. The tex-

tiles made of porous iPP exhibit a higher moisture uptake and a higher gas transport. It follows that the β -form iPP possesses a potential practical applicability.

However, the β -form iPP occurs much more rarely than does the predominant α -form under most conditions. Previous studies were concentrated on the technique that obtains a higher level of the β -form and on the morphological structure of the β -form. Several techniques have been developed, but among the more commonly used are the following:

1. Additions of certain heterogeneous nuclei.⁶⁻⁹
2. Crystallization in a temperature gradient.¹⁰
3. Shear-induced β -form crystallization.¹¹

In general, the contents of the β -form produced by the latter two methods are smaller than those produced by the former. Moreover, β -spherulites homogeneously dispersed in the bulk sample rather

* To whom correspondence should be addressed.

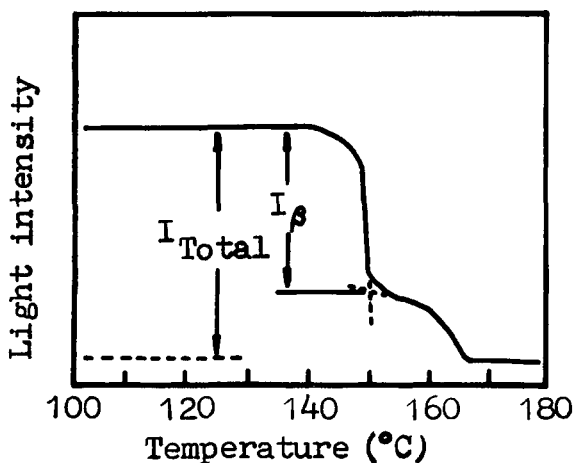


Figure 1 Typical melting scan of the iPP containing both β - and α -crystalline forms.

than only in the skin as in the shear-induced method.¹¹

Quinacridone dyestuff Permanent Red E3B, which was developed by Leugering in 1967,⁶ has proved to be useful for inducing the β -form iPP. The Kx value, calculated from an empirical ratio proposed by Jones et al.,³ is up to 0.73 for the sample containing ca. 0.00001 wt % of the E3B. In the early 1980s, a low molecular weight compound denoted by DACP was found to be more effective than was the E3B. The corresponding Kx is as high as 0.93. Other additives described in the literature are less effective than the aforesaid additives.⁷ Thus far, only a few compounds could serve as the β -nucleator. Although the β -form iPP has been investigated thoroughly, little is known about the β -nucleator. Our goal in this study has been to extend and clarify the earlier investigations so as to better understand the chemical and physical characters of β -nucleators. We also sought to investigate the morphology and optimum growth conditions of β -spherulites.

In the course of this study, several more effective β -nucleators were developed by melt crystallization under suitable conditions. By adding a small amount

of these β -nucleators, the iPP samples with the β -form crystallinity content as high as 0.95 characterized by Kx were obtained. Few α -form spherulites could be observed under a polarizing microscope (PLM) and a scanning electron microscope (SEM) with these samples. The effects of the nucleator concentration, cooling rate, crystallization temperature, and melt temperature on the β -form level were studied with a view of finding out the optimum growth condition of β -spherulites. Furthermore, the analysis of particle shape and structure of the nucleators were given with the purpose of revealing the correlations of these features with β -form levels. Observations of the morphological structure of β -spherulites were also carried out.

EXPERIMENTAL

Materials

Isotactic polypropylene (iPP) with a melt flow index of 19 g/10 min from Liaoyang Chemical Works of Liaoning Province in China was used for all tests. Organic dyes as β -nucleators were kindly supplied by the Dyeing and Finishing Group of China Textile University. Other materials selected as β -nucleators were chemically pure and commercially available. No further treatment was done to all these materials before use.

Sample Preparation

All additive-containing iPP samples were obtained by blending iPP chips with small amounts of additives, followed by thorough agitation to assure uniform dispersions. The concentrations of the additives varied from 0 to 0.1 wt %.

Hot-Stage Method

The additive-containing iPP was sandwiched between glass slides and then put on a hot stage.

Table I Physical Properties of Inorganic Additives and Kx Values of the iPP Containing the Additives of 0.1 Wt %; the iPP Samples Were Prepared by Sand-Bath Method

Additive	Appearance	Crystalline Form	MP (°C)	Kx
ZnO	White powder	Hexagonal	1975	0.06
CaCO ₃	White powder	Hexagonal or triclinic	825 (Dec)	0.15
NaNO ₃	Crystal	Pseudo-hexagonal	308	0.13
NaCl	White crystal	Cubic	804	0
No additive				0.36

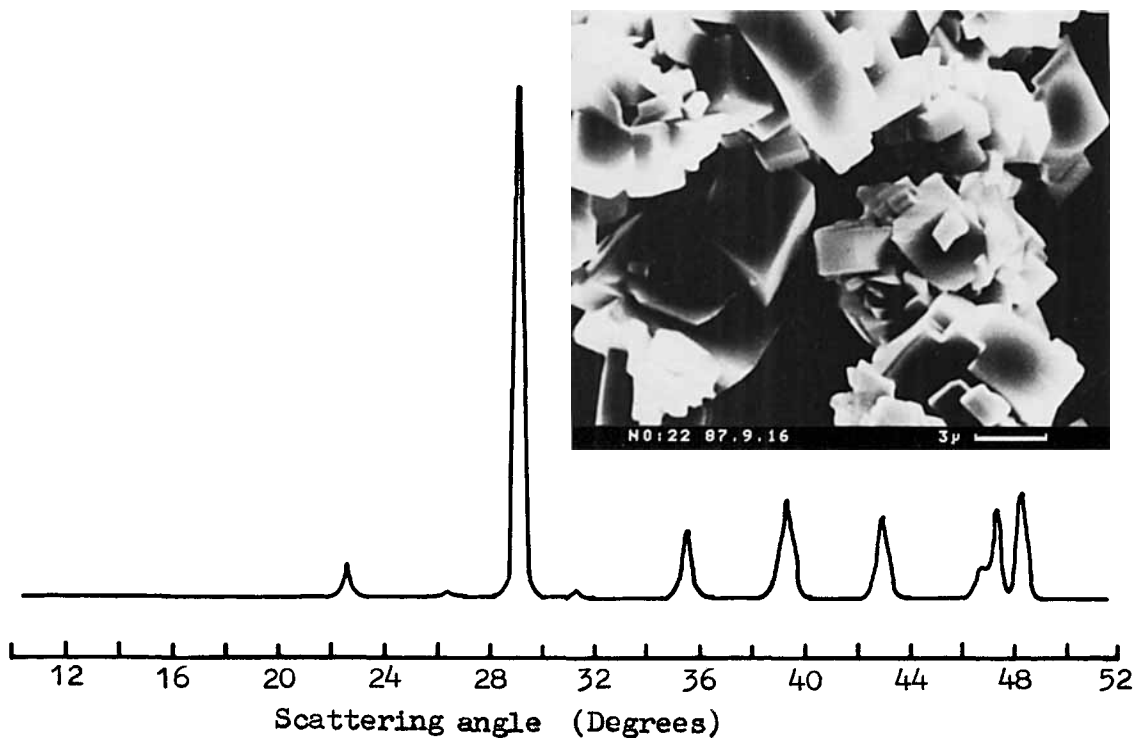


Figure 2 X-ray diffraction diagram and scanning electron micrograph of CaCO₃.

After the iPP had melted, it was kept at 200°C for 10 min. Then, the hot stage was unplugged to allow it to cool down to 50°C at a cooling rate of ca. 8°C/min.

Sand-Bath Method

The additive-containing iPP was put in a glass vessel that was immersed in sand in advance, then heated to 200°C. Following the hold period at 200°C for 30 min, the iPP was allowed to cool down to 50°C at the cooling rate of ca. 2°C/min.

Isothermal Crystallization Method

The additive-containing iPP was sandwiched between two glass slides and put on a hot stage at 200°C. After the iPP had molten completely, it was quenched rapidly into either a fluid of high-heat capacity—water from 0 to 100°C—or glycerine above 100°C to crystallize for 10 s or 2 h. After this period, the iPP was taken out and cooled in ice water.

X-ray Diffraction

X-ray diffraction patterns were recorded using a Rigaku 3015 X-ray diffractometer equipped with a copper target and nickel filter. The X-ray pho-

tograph was taken with a flat-film camera, sample-to-film distance of 30 mm, and exposure time of 2 h.

Kx values representing the relative levels of the β-form iPP were calculated using the Turner-Jones eq. (1) based on a typical X-ray diffraction diagram:

$$Kx = H(300)/[H(300) + H_{\alpha}] \quad (1)$$

where H(300) is the height of the peak from the β-form at 2θ = 16.2, and H_α, the total height of the peaks from the α-form at 2θ = 14.2, 17.0, and 18.8. The order parameter S of the β-form was calculated by eq. (2):

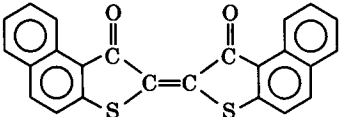
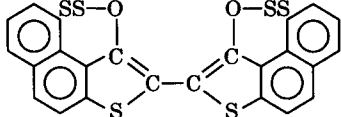
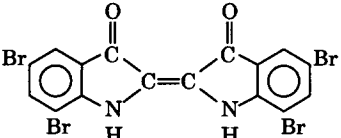
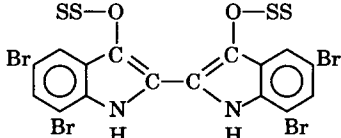
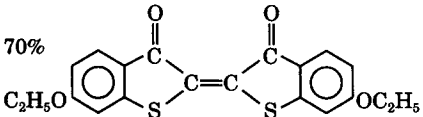
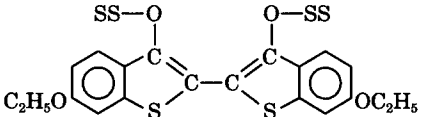
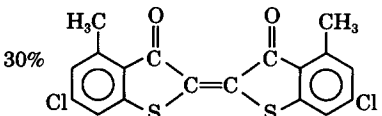
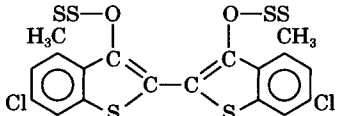
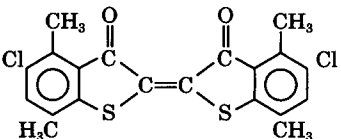
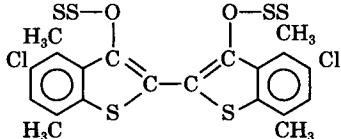
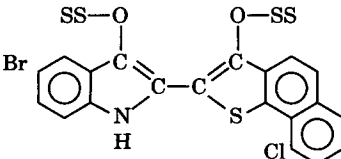
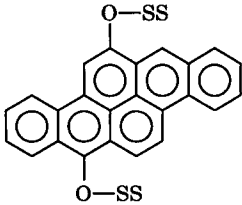
$$S = H(300)/[H(300) + H(301)] \quad (2)$$

where H(301) is the height of the peak from the (301) crystalline face of the β-form. The higher the S value is, the higher the order of the β-form.

Depolarized Light Intensity

Depolarized light intensity (DLI) scans were recorded using a DLI-1 type depolarized light meter equipped with a hot stage made at the China Textile

Table II Structure of Organic Additives and Kx Values of the iPP Containing 0.05 Wt % Additives; "SS" Represents the Sulfonic Sodium Group

Additive Name (Shape)	Kx^a	Additive Name (Shape)	Kx^a
Indanthren Brown RRD (lumps)	0.07/0.04	Indigosol Brown IRRD (rods)	0.46/0.54
			
Durindone Blue 4BC (needles)	0/0	Cibantine Blue 2B (lumps)	0.15/0.86
			
Algol Scarlet GGN (needles)		Cibantine Orange HR (plates)	0.45/0.82
70% 			
+		Indigosol Pink IR (plates)	
30% 	0.22/0.07		(0.62/0.82)
Ciba Red F2B (needles)	0.26/0.46	Indigosol Red Violet IRH (plates)	(0.46/0.68)
			
No additive	0.03/0.36	Indigosol Grey/IBL (lumps)	0.56/0.95
			
		Indigosol Golden Yellow IGK (lumps)	0.48/0.92
			

^a Kx values from the iPP samples prepared from the hot-stage method and the sand-bath method, respectively.

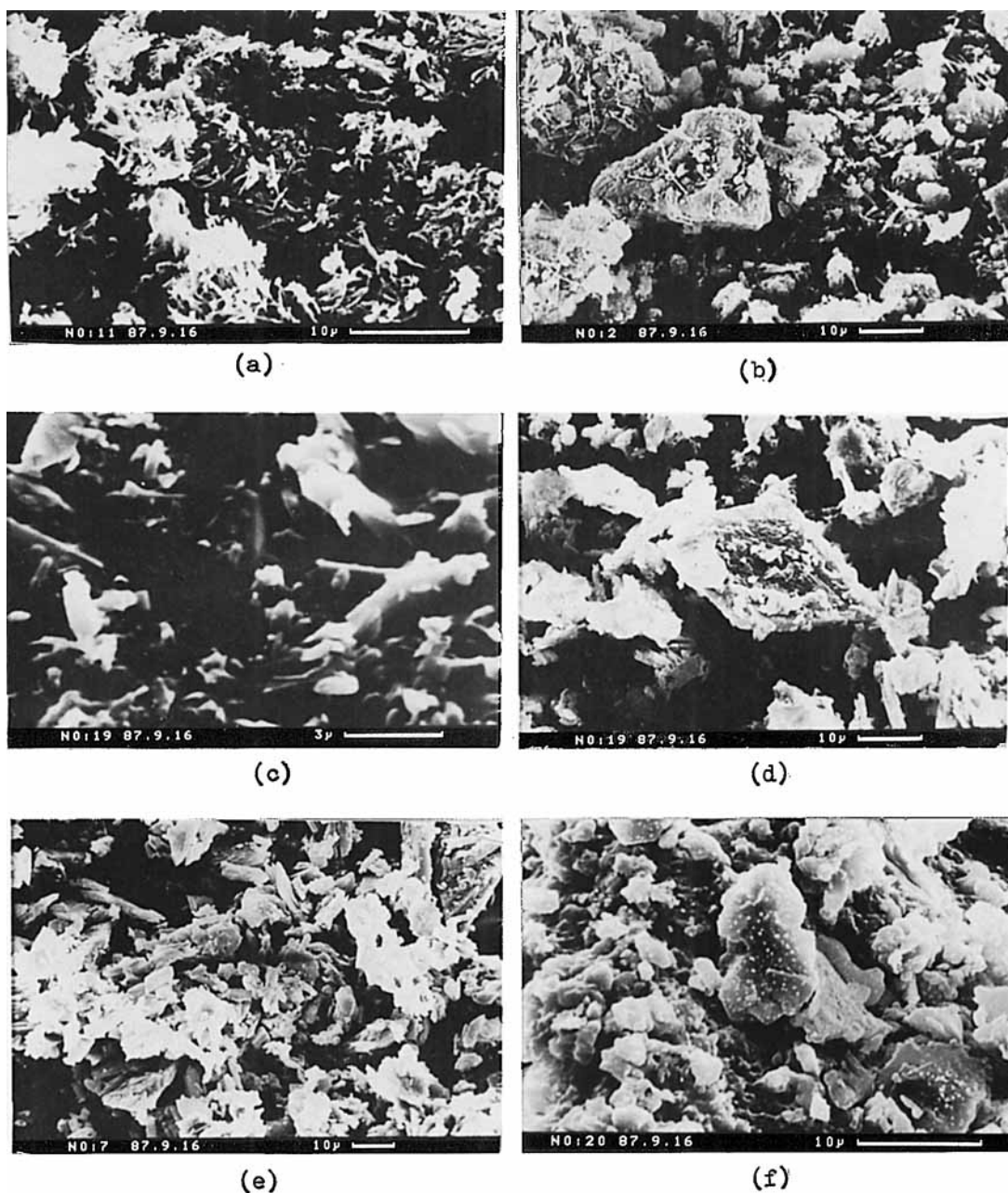


Figure 3 Typical SEM micrographs of additives: (a) Algol Scarlet GGN; (b) Ciba Red F2B; (c) Indigosol Brown IRRD; (d) Indigosol Red Violet IRH; (e) Cibantine Orange HR; (f) Indigosol Grey IBL.

University. A representative melting DLI scan is shown in Figure 1. The K_{DLI} values representing the relative amounts of the β -form iPP were determined by taking the ratio

$$K_{DLI} = I_{\beta}/I_{total} \quad (3)$$

where I_{β} is the light intensity change due to the melting of the β -phase, and I_{total} , the total light in-

tensity change following complete melting of the sample.

Polarizing Microscope

Polarizing light micrographs were taken on a Wild Leitz polarizing microscope. For transmission microscopy with polarized light, the iPP samples were sectioned into thin films with a microtome and

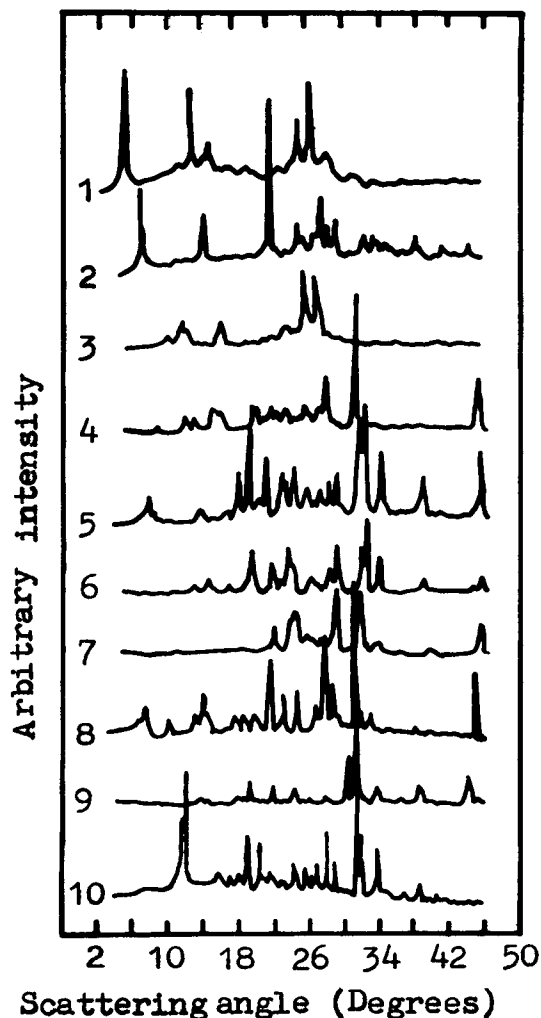


Figure 4 X-ray diffraction diagrams of the 10 additives. For numbers, refer to Table III.

mounted between glass slides, together with a drop of glycerin.

Scanning Electron Microscope

Scanning electron microscope (SEM) photographs were taken on a Cam-Scan high-resolution SEM Model 4. For a morphological study of β -form spherulites, the iPP samples prepared by the sand-bath method were etched in the mixture solution of $\text{H}_2\text{SO}_4/\text{H}_2\text{O}/\text{CrO}_3$ (20 mL/80 mL/50 g) for 5–20 min after swelling with decalin for 3–5 min at 80°C. Then, the samples were washed, dried, and plated with gold.

Small-Angle Light Scattering

The small-angle light scattering (SALS) patterns of the iPP samples prepared by the isothermal crys-

tallization method were taken on a SALS instrument made at the China Textile University. A continuous-wave He—Ne laser was used as the polarized, monochromatic light source. A 1 mm pinhole was placed behind the samples. The distance between the sample and a negative film was ca. 11 cm.

RESULTS AND DISCUSSION

Selection of β -Nucleators

It is assumed that the compounds with a hexagonal or pseudo-hexagonal crystallinity might help to induce the β -form iPP. Several inorganic additives listed in Table I were incorporated in iPP with the concentration of 0.1 wt % before the iPP crystallized in the sand bath. Unfortunately, X-ray diffraction analyses gave Kx values of less than 0.15 for the iPP containing the inorganic additives, indicating that a minority of the β -form constituents were present. The Kx values are even lower than that of the iPP without additives ($Kx = 0.36$). This crystallization behavior appears to be related to the abilities of the additives accelerating the growth of only the α -form. If the growth of the α -form spherulites nucleated at a higher temperature was accelerated to an adequate speed by the additives, they could grow to impingement before the β -spherulites nucleated at a lower temperature began to crystallize. Thus, the growth of the β -spherulites was repressed.

On the basis of the crystalline form of the above additives, the reason that calcium carbonate is unable to induce the β -form crystallinity may be that its crystalline form is not hexagonal according to the X-ray diffraction diagram and SEM photograph shown in Figure 2. Even if the crystalline form of the additive is hexagonal, the β -form iPP was not necessarily induced, as in the case of zinc oxide as the additive. This is probably due to the smaller dimension of the zinc oxide crystalline cell ($a = 3.24 \text{ \AA}$, $c = 5.20 \text{ \AA}$) than that of the β -form cell ($a = 19.08 \text{ \AA}$, $c = 6.49 \text{ \AA}$).³

Further, a series of organic additives were incorporated into iPP before the iPP crystallized from the melt by the hot-stage or sand-bath method. The Kx values given in Table II illustrate that the substantial β -form could grow in the presence of most organic additives. The maximum Kx value can reach to 0.95 when the iPP sample contains 0.05 wt % Indigol Grey IBL. In looking at Table II, one can find that for the most organic additives the β -form levels of the iPP prepared by the sand-bath method are much higher than are those by the hot-stage

Table III WAXD Data of the Additives and Kx Values of 0.05 Wt % Additive-containing iPP Prepared by the Sand-bath Method

No.	Additive Name	d -Spacing (\AA)		Kx
		Strongest/Second Strongest		
1	Indanthren Brown RRD	16.1/3.38		0.04
2	Durindone Blue 4BC	4.06/10.8		0
3	Algol Scarlet GGN	3.49/3.33		0.07
4	Indigosol Brown IRRD	2.83/3.16		0.54
5	Cibantine Blue 2B	4.67/2.83		0.86
6	Cibantine Orange HR	2.81/3.08		0.82
7	Indigosol Pink IR	3.07/2.82		0.82
8	Indigosol Red Violet IRH	2.83/3.19		0.68
9	Indigosol Grey IBL	2.84/2.94		0.95
10	Indigosol Golden Yellow IGK	7.37/2.83		0.92

method. This is obviously related to the cooling rate during the β -form growth. It is known that a lower cooling rate would favor the crystallization of the β -form, owing to its lower rate of nucleation and higher rate of growth in comparison with the α -form. Further discussion about this point will be given in more detail.

It is noteworthy that the additives in the right vertical column of Table II are much more effective than are those in the left column with respect to the ability of inducing the β -form. Based on the molecular struc-

ture of these additives, the difference between the left and right columns can be illustrated by

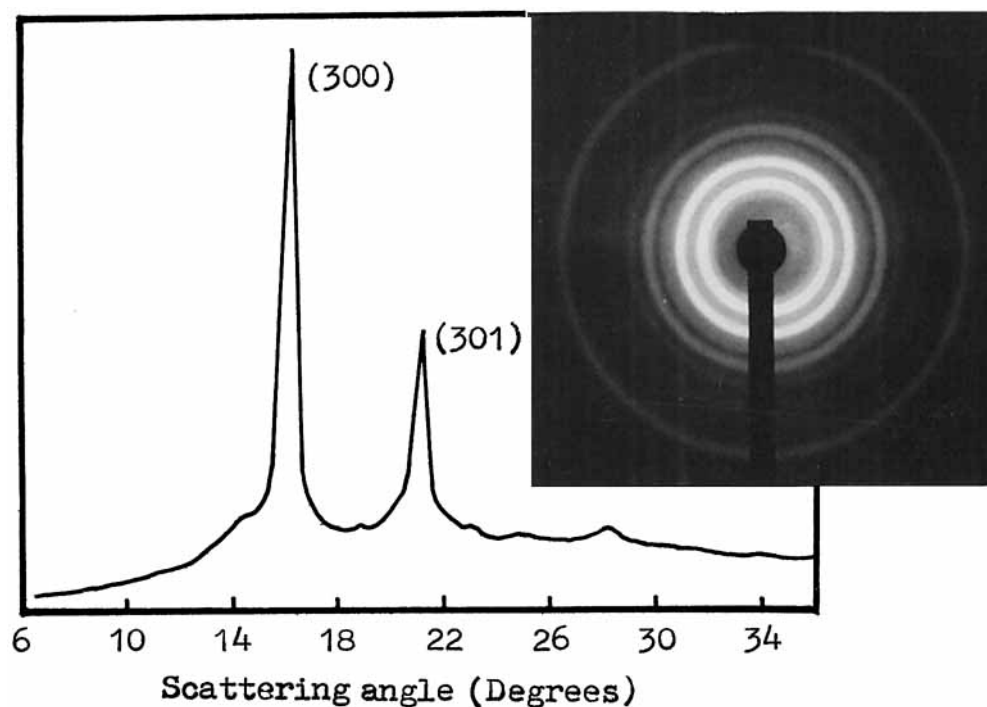
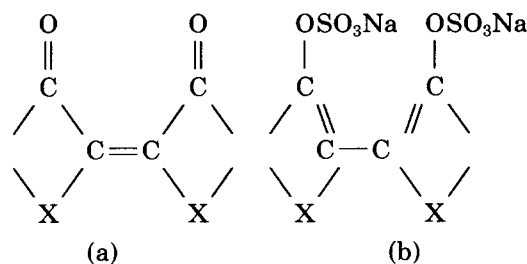


Figure 5 X-ray diffraction patterns of overwhelming β -form iPP with the Kx value of 0.95. The β -nucleator is Indigosol Grey IBL.

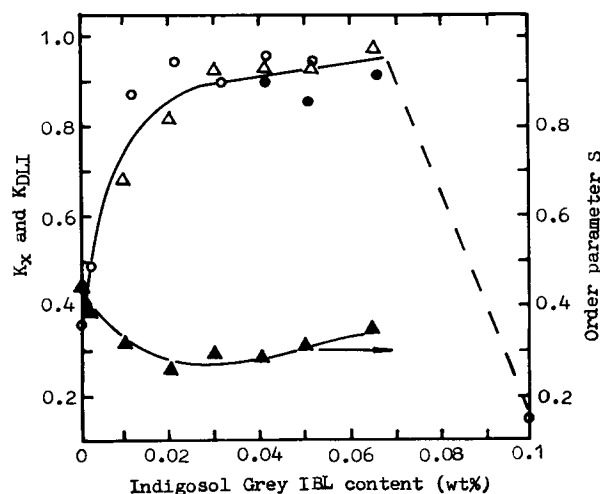


Figure 6 Dependencies of K_x , K_{DLI} , and order parameter S values on Indigosol Grey IBL concentration in the iPP prepared by the sand-bath method: (○) K_x , (△) K_{DLI} , and (●) K_x of the hot-stage samples.

where $X = S$ or NH . It might be inferred that the presence of the sulfonic sodium group might enhance the ability of inducing the β -form. It has been suggested that the additives having the sulfur atom in or above the phenyl ring can induce the β -form.⁷ For instance, triphenodithiazine, phenothiazine, and anthraquinone-2,6-disulfonic sodium can induce the β -form but of a lesser magnitude. The K_x values of the iPP samples prepared by the hot-stage method are 0.28, 0.08, and 0.05, respectively. Nonetheless, Permanent Red E3B, without the sulfur atom, can also serve as an effective β -nucleator with the K_x value of ca. 0.73.⁸ It follows that the presence of the sulfur atom is not key factor for inducing the β -form.

It can be seen from Table II that all the effective β -nucleators show a mutual molecular structure, namely, the fused ring structure. However, all additives with the fused ring structure cannot act as effective β -nucleators. Indanthren Rubine R, Indanthren Red F3B, and Eliamina Yellow RR, e.g., have their corresponding K_x values of 0.03, 0.03, and 0.07, respectively. (These three iPP samples were prepared by the hot-stage method.) It is more unsatisfactory that both Indigo N and Durindone Blue 4BC have the corresponding K_x values of 0, indicating that they would repress the growth of the β -form. It is difficult to determine the close relationship between the molecular structure and the ability of inducing the β -form, but the structural character of the fused ring seems to be necessary for the additives suitable for inducing the β -form.

Perhaps the other factor that affects the level of the β -form is the shape of the additive.⁷ As seen in Table II and Figure 3, the additives with needle shapes tend to repress or not favor the growth of the β -form, whereas those with plate or lumpish shapes would favor the growth of the β -form with the exception of Indanthren Brown RRD. However, the particle shape cannot reflect well the fine crystalline form of the additives, since the exterior condition would affect the particle shape during the crystal growth. To make up this deficiency, X-ray diffraction measurements of these additives were carried out, and the results are presented in Figure 4 and Table III. It is evident that the additives that exhibit the strongest or second-strongest reflections at a d -spacing of 2.83 Å possess corresponding K_x values higher than 0.54, while those without these specific reflections possess relatively low K_x values. It seems that there is a close relation between this specific reflection and the β -form level, i.e., those additives having the strongest or second-strongest diffraction peaks at the d -spacing of ca. 2.83 Å could serve as highly effective β -nucleators.

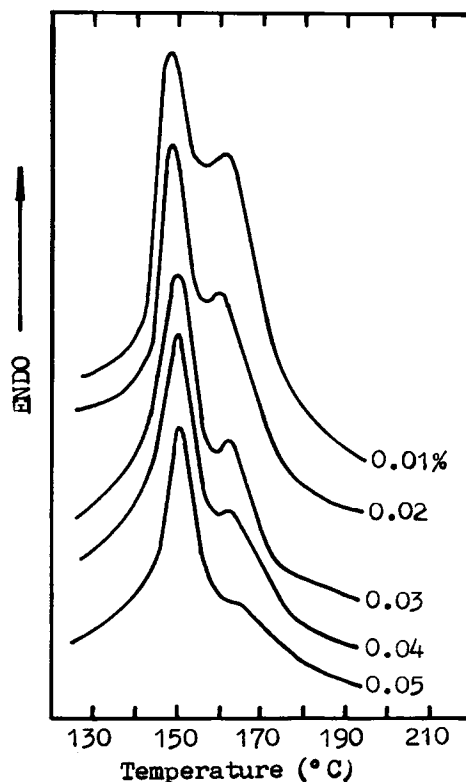


Figure 7 DSC traces of the iPP with varied Indigosol Grey IBL concentrations (as indicated by curves) at a heating rate of 20°C/min. The iPP was obtained by allowing the IBL-containing samples to crystallize from the melts of 200°C at a cooling rate of 5°C/min.

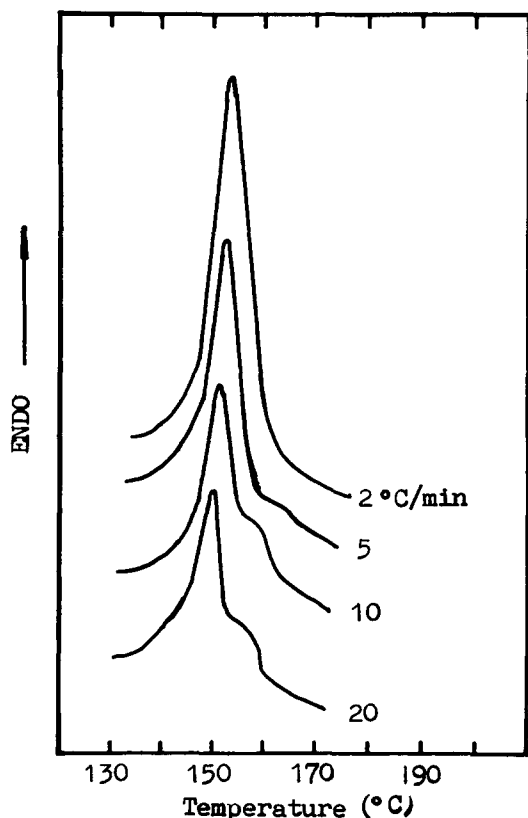


Figure 8 Effect of cooling rate on melting behavior of overwhelming β -form iPP at a heating rate of 20°C/min. The test samples were obtained by allowing the IBL-containing iPP to crystallize from 200°C melt with the respective cooling rates indicated at the curves.

It must be appreciated that the d -spacing of the strongest reflection of the β -form is 5.644 Å, which is approximately the double of 2.83 Å. What on earth does this quantitative relationship mean? This problem is a subject for further studies.

Summarizing, then, the most effective β -nucleator in this study is Indigosol Grey IBL, which causes the molecular chains to alter their packing mode from the monoclinic α -type unit cell to the hexagonal one of the β -form. This is confirmed by the X-ray diffraction patterns shown in Figure 5. It can be seen that the diffraction peaks of the (300) and (301) planes of the β -form crystallinity are very strong, whereas another three diffraction peaks of the α -form almost disappear, suggesting that the iPP sample is essentially free of the α -form.

Effect of Crystallization Conditions on β -Spherulite Growth

Here, emphasis is given to the influence of variables, such as nucleator concentration, cooling rate, crys-

tallization temperature, and melt temperature, and melt temperature, on the resultant β -form level. As seen in Figure 6, the X-ray diffraction analyses give the Kx values to increase steeply with the Indigosol Grey IBL concentration varying from 0 to 0.02 wt %, then keep constant at ca. 0.93 in the range of 0.02–0.07 wt %. An analogous change can be observed in the relation of K_{DLI} to the β -nucleator concentration shown in Figure 6. This is evident from DSC scans shown in Figure 7, in which all the iPP samples containing various nucleator concentrations exhibit a sharp and narrow endotherm when they were heated at a heating rate of 20°C/min. The large endotherms peaking at 151°C are due to the melting of the β -phase crystals. The high-temperature shoulders at 162°C are due to the melting of the α -phase crystals. With increase of the nucleator concentration from 0.01 to 0.05 wt %, the shoulder peak decreases and eventually disappears, which confirms the higher β -phase purity in the iPP sample containing 0.05 wt % Indigosol Grey IBL. If, however, the β -nucleator concentration is further increased to 0.1 wt %, the Kx value would decrease steeply to 0.15. It follows that the optimum concentration of this β -nucleator is 0.03–0.07 wt %. It was reported that the optimum concentrations of Permanent Red E3B and DACP were 10⁻⁵ and 0.1 wt %, respectively.^{8,9}

On the other hand, order parameters do not essentially change in the range of 0.01–0.06 wt % of the nucleator concentration (Fig. 6), indicating that little change of the morphological structure occurs.

To investigate the effect of the cooling rate on the β -form iPP level, the samples with 0.05 wt % Indigosol Grey IBL were allowed to crystallize from the melt at 200°C at the respective cooling rates of 2, 5, 10, and 20°C/min in DSC. The re-

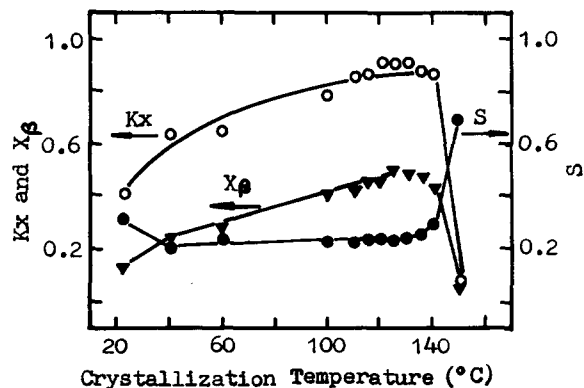


Figure 9 Kx , X_{β} , and S vs. crystallization temperature for the iPP containing 0.04 wt % Indigosol Grey IBL. The crystallization time was 2 h.

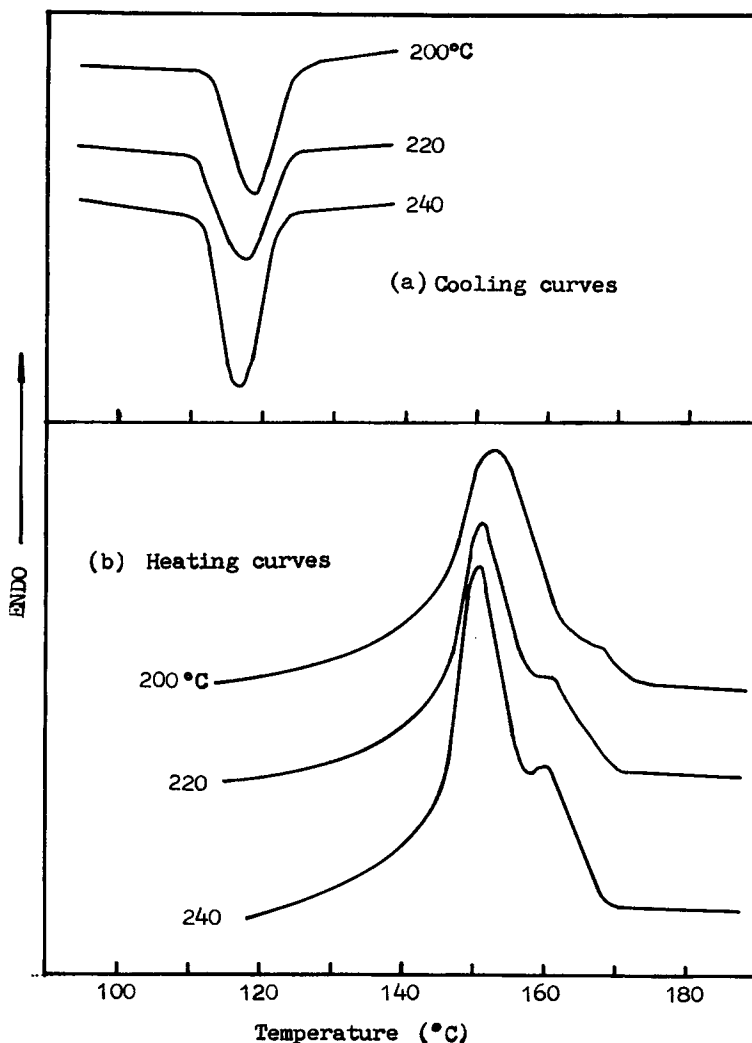


Figure 10 Effect of melt temperature (as indicated at curves) on thermal behavior of overwhelming β -form iPP: (a) cooling traces at a cooling rate of $5^\circ\text{C}/\text{min}$; (b) the subsequent melting traces at a heating rate of $20^\circ\text{C}/\text{min}$.

sulting iPP samples have the anticipated thermal properties with subsequent melting presented in Figure 8. The high-temperature shoulders attributed to the melt of the α -phase diminished gradually and eventually vanished, while the lower-temperature peaks attributed to the melt of the β -phase enlarged gradually with a decreasing cooling rate from 20 to $2^\circ\text{C}/\text{min}$. The lower cooling rate is favorable for growth of the β -form iPP, which coincided with the result with DACP serving as the β -nucleator.⁹ This behavior further accounts for the differences of Kx values between the hot-stage and sand-bath samples.

The dependence of Kx values on crystallization temperature (T_c) for isothermal crystallization samples is presented in Figure 9. It is noted that the

maximum Kx value locates at 125°C , suggesting that the β -form grows to a significant portion at this temperature. Jacoby et al. also noted that the temperature at which the β -spherulites began nucleating and rapidly grew to encompass a significant portion of the field of view under a polarizing light microscope was 126°C .⁸ This is because, in the temperature range of 122 – 138°C , the β -spherulites grow ca. 20–70% faster than do the α -spherulites.

Similar T_c dependence of the relative crystallinity (X_β) of the β -form crystal is observed in Figure 9. The X_β is based on comparison of the β -form to the total crystallinity plus amorphous content, expressed as follows:

$$X_\beta = A_\beta / (A_\beta + A_\alpha + A_a) \quad (4)$$

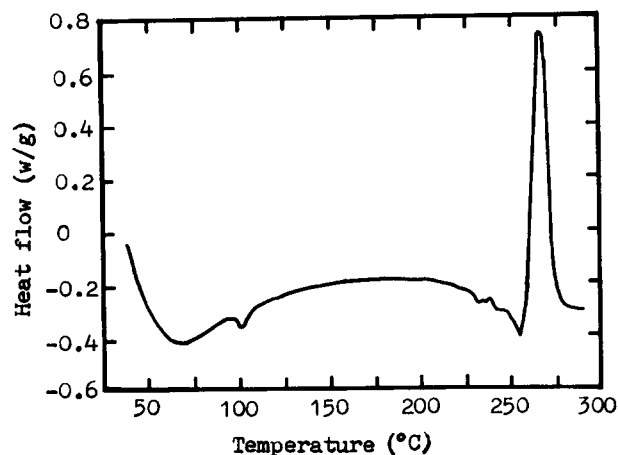


Figure 11 DSC diagram of Indigosol Grey IBL at a heating rate of 20°C/min.

where A_β , A_α , and A_a are the areas under the β -form (300) peak, α -form (110), (040), (130) peaks, and the amorphous content, respectively. It can be seen from Figure 9 that the higher the Kx value the higher the X_β value is. The highest X_β value can reach up to about 0.5 at the T_c of 125°C. Moreover, the amorphous content at this T_c is the lowest. The fact that both the Kx and the X_β values reach the maximum values at the same time is expected, especially when looking at the material's performance.

Nevertheless, the order parameter S of the β -form hardly changes with the increase of T_c until 140°C. This is probably due to that the crystallization time

is long enough to eliminate the effect of T_c on the order parameter. The jump of this order parameter above 140°C might be associated with the rapid decline of the β -form level.

To study the effect of melt temperature on the β -form level, the iPP specimens containing the β -nucleator were heated to above 200°C. After being held at 200°C for 10 min, the specimens were allowed to crystallize at a cooling rate of 5°C/min. Finally, the DSC measurement for the specimens was performed at a heating rate of 20°C/min to detect the level of the β -form. The cooling and heating DSC traces are shown in Figure 10. Although the cooling traces exhibit almost the same crystalline enthalpy and temperature, the subsequent melting traces show a discrepancy for the specimens subjected to different melt temperatures. As seen in Figure 10(b), the melting peaks of the α -phase crystals become appreciable as the melt temperature increases, indicating that α -form crystals have formed. This could be explained by the thermal property of Indigosol Grey IBL shown in Figure 11. Melt temperature higher than 240°C would destroy the partial nucleation of this nucleator.

In summary, the optimum growth conditions of the β -form iPP are the following:

1. The concentration of Indigosol Grey IBL in iPP should be controlled in the range of 0.02–0.07 wt %, and the most suitable concentration seems to be 0.04 wt %.

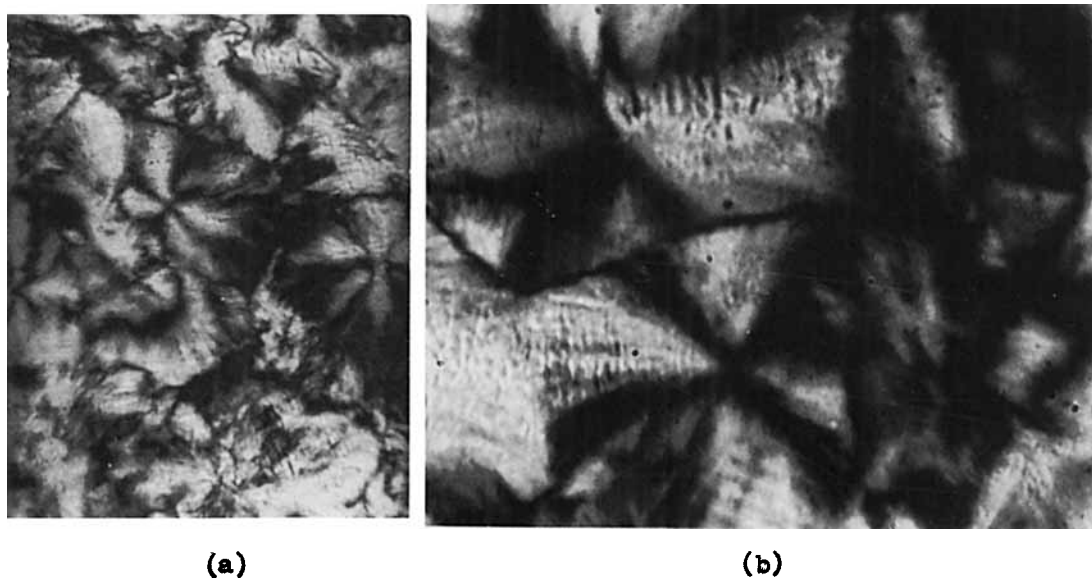


Figure 12 Polarizing micrographs of overwhelming β -form iPP ($Kx = 0.95$) with Indigosol Grey IBL as the β -nucleator. Magnifications: (a) 100; (b) 400.

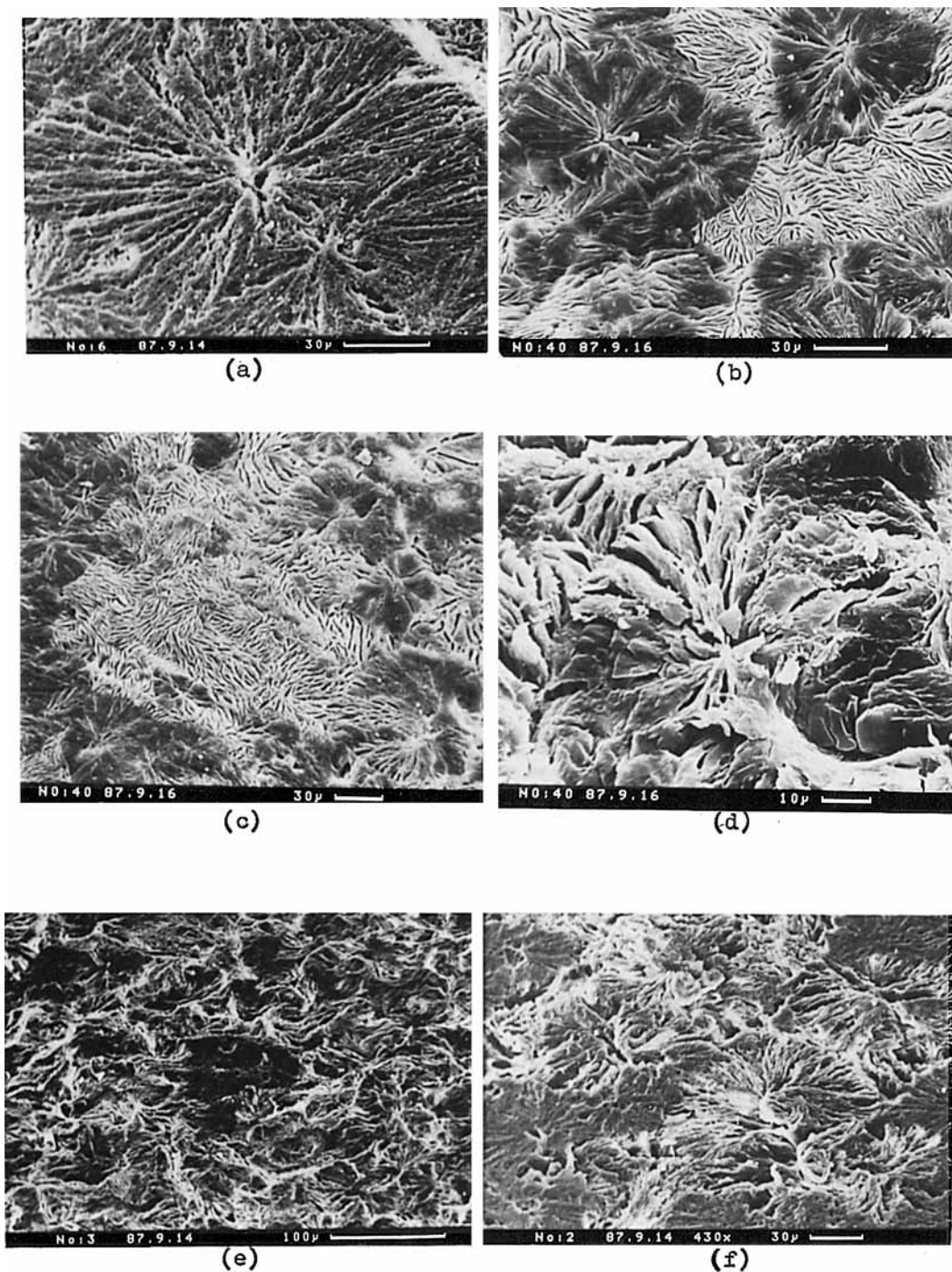


Figure 13 SEM micrographs of etched specimens of iPP: (a) α -Spherulites at etching time of 20 min; (b) α - and β -spherulites at etching time of 10 min; (c) twistable β -spherulites at etching time of 10 min; (d) β -spherulites (high magnification) at etching time of 10 min; (e) sheaflike β -spherulites at etching time of 20 min; (f) sheaflike β -spherulites (high magnification) at etching time of 20 min.

2. The cooling rate should be controlled to be no higher than $5^{\circ}\text{C}/\text{min}$ when an anisothermal crystallization is employed.

3. The crystallization temperature should be controlled at ca. 125°C when an isothermal crystallization is employed.

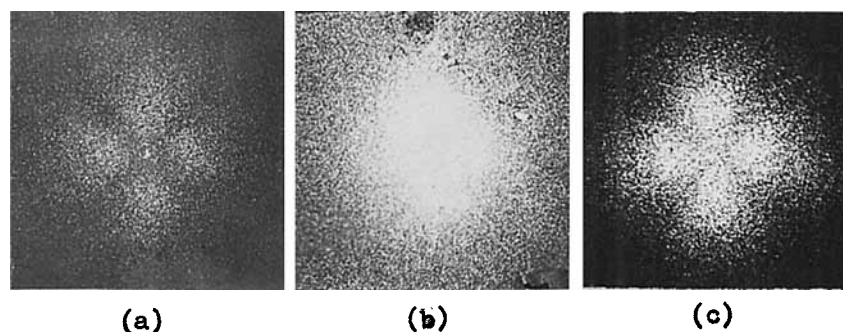


Figure 14 Typical change in Hv small-angle light-scattering patterns from the Indigosol Grey IBL-containing iPP crystallized for 10 s at crystallization temperatures (a) 26°C, (b) 90°C, and (c) 100°C.

- The melt temperature should be controlled to be no higher than 220°C.

In this way, a predominately β -form iPP could be attained.

Morphological Structure of β -Spherulites

The morphological structures of the iPP samples with different levels of β -form spherulites were studied by a polarizing microscope. The views of the iPP containing both β - and α -spherulites under a polarizing microscope show bright color and dark regions. It is convenient to classify the bright and the dark spherulites as β - and α -forms, respectively, according to previous studies.¹² The high luminosity of β -spherulites is attributed to higher birefringence values in comparison with α -spherulites. For the specimen containing a medium level of the β -form, the β -spherulites exhibit a columnar structure. There is an explicit boundary between α - and β -spherulites, suggesting their aggregation separately. This oriented growth manner of β -spherulites is in agreement with the manner of iPP growth when E3B serves as the β -nucleator.⁸ However, the discrepancy occurs in the dark areas, i.e., the shapes of some α -spherulites change from quasi-parabolic to teardrop-like shapes. This behavior appears to be related to the matrix in which α -nuclei grow. When the matrix is of the α -phase, the spherulites resulting from α -nucleation will adopt the usual quasi-parabolic shape.¹⁰ If, however, the matrix changes from the α - to the β -phase, the α -spherulite shape would also change from quasi-parabolic to teardrop-like. The transformation of the α -spherulite shape results from the fact that β -spherulite can prevail over the α -mode of growth and eventually overtake it, owing to the faster growth rate of the β -spherulite. If iPP is zone-solidified in a temperature gradient, the α -

spherulites within the β -matrix would adopt more explicit teardrop-like shapes.¹⁰

There are two morphological structures of β -spherulites: One appears as a Maltese Cross, and the other also as a Maltese Cross, but also displays some concentric banding of a rather spiky, jagged character (see Fig. 12). The former is Type III, and the latter, Type IV, according to previous studies. The morphological structures of the β -spherulites are similar to those reported in the literature.^{13,14} In our experiments, the overwhelming proportion of β -spherulites exhibiting the Maltese Cross have a rather spiky, jagged character (Type III) and a few exhibit the normal Maltese Cross (Type IV).

Further observations were made for the fine structure of etched samples by SEM. Figure 13 shows the morphological structure of α - and β -spherulites. α -Spherulites exhibit conventional central nucleating entities which initiate crystal growth in all directions. This is depicted by Figure 13(a)–(c) and (e). In Figure 13(b) and (c), the lamellar structure of β -spherulites is also revealed, indicating their twistable structure character. Figure 13(d) shows the lamellar structure in high magnification, suggesting that dendritic growth has occurred. If the etching time was prolonged to 20 min, the sheaf-like features of β -spherulites can be clearly observed [Fig. 13(e) and (f)]. One can imagine that β -spherulite develops from one single crystal through essentially unidirectional growth. The spherical shape is attained through continuous branching and twisting via the intermediate stage of sheaves. Such branching and twisting lamellae are responsible for the color character under a polarizing microscope due to the different retardations produced by such a lamellar structure and also accounts for lower values of the modulus and yield stress and higher values of elongation at break and impact strength of β -iPP.

SALS experiments were carried out to study the superstructure of β -spherulites. Figure 14 shows typical Hv SALS patterns for the iPP samples containing 0.04 wt % Indigosol Grey IBL. The four-lobe patterns are typical of the patterns observed from α -spherulites.¹⁵ The Hv SALS patterns of the iPP samples become smaller gradually as crystallization temperature increases from 2 to 70°C. At the crystallization temperature, T_c , of 80 and 90°C, the Hv pattern changes from four-lobe to round. If T_c further increases from 90 to 130°C with a step of 10°C, the resulting Hv SALS patterns change back to the four-lobe patterns and their sizes are almost the same. The change of the patterns at 80 and 90°C appears to be related to the transformations of crystalline forms. It has been found that β - and α -form crystallinities have different crystallization kinetics. β -Spherulites nucleated at a much lower rate than did α -spherulites, but once nucleated, they grow faster by 20–70%. These two opposing trends have the consequence that β -spherulites occur only in the suitable T_c range. In this study, this suitable range is 20–145°C when β -spherulites can be induced by Indigosol Grey IBL and the crystallization time is 2 h (see Fig. 9). If, however, the crystallization time

is shortened to 10 s, this T_c range would become narrow.

On the basis of the onset of the transition from dark to luminous dots under a polarizing microscope, we can determine that the limited lower T_c is at 80°C at which β -spherulites become appreciable. Therefore, the round Hv patterns at 80 and 90°C result from the small β -spherulites just grown. The vague outline is due to the incomplete superstructure of β -spherulites. At fixed T_c , with the prolongation of crystallization time from 10 to 60 s, their Hv SALS patterns would become more distinct (Fig. 15), suggesting that sufficient time is required to modify the β -spherulite structure. However, if crystallization time is prolonged for another 60 s, the four-lobe pattern would become somewhat vague [Fig. 15(c)]. This phenomenon is probably due to the formation of β -spherulite aggregates during a long period, owing to the higher growth rate of the β -spherulites.

CONCLUSIONS

A series of iPP specimens containing varying levels of β -form crystallinity have been prepared by intro-

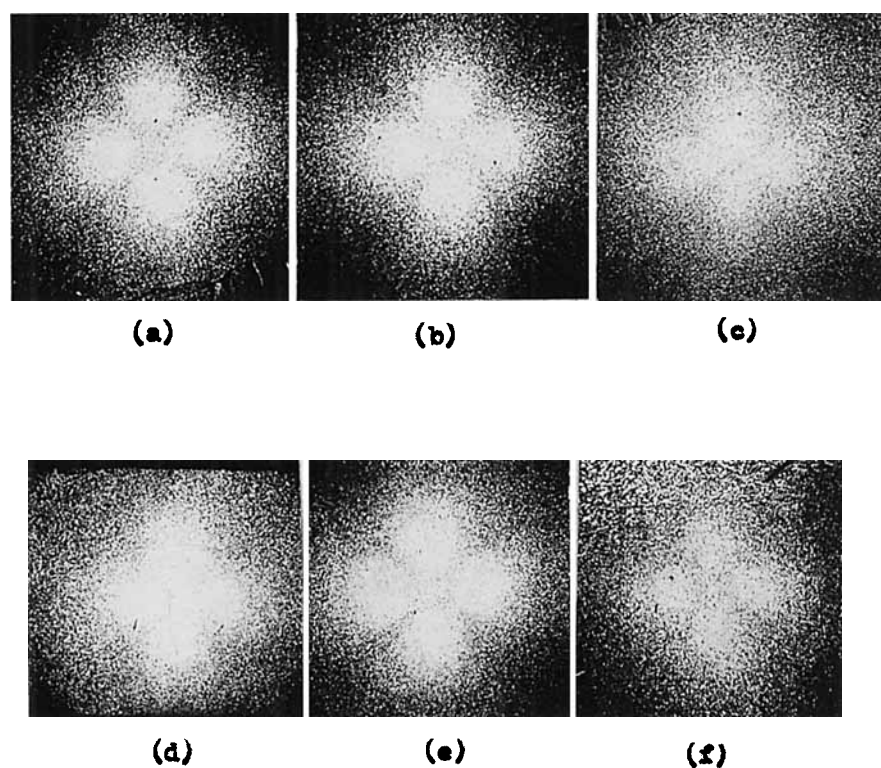


Figure 15 Hv small-angle light-scattering patterns from Indigosol Grey IBL-containing iPP at different crystallization temperatures and times: (a) 130°C, 30 s; (b) 130°C, 60 s; (c) 130°C, 120 s; (d) 137°C, 10 s; (e) 137°C, 20 s; (f) 137°C, 60 s.

ducing different additives. It has been found that Indigosol Brown IRRD, Indigosol Red Violet IRH, Cibantine Orange HR, Indigosol Pink IR, Cibantine Blue 2B, Indigosol Golden Yellow IGK, and Indigosol Grey IBL are more effective β -nucleators. The respective Kx values of the iPP containing the seven nucleators are in the range of 0.54–0.95. These more effective β -nucleators have been found to show a mutual characteristic in that the strongest or the second-strongest reflections locate at a d -spacing of ca. 2.83 Å in their X-ray diffraction diagrams. Additional mutual characteristics are their fused benzene ring and heterocycle structures. The presence of the sulfonic sodium group above the fused ring can largely enhance the ability of inducing the β -form iPP.

The predominately β -form iPP would be expected to be favored by the optimum β -nucleator concentration of 0.02–0.07 wt %, the lower cooling rate of less than 5°C/min during an isothermal crystallization, or the optimum crystallization temperature of ca. 125°C during isothermal crystallization and the optimum melt temperature of no higher than 220°C. Morphological studies on β -form crystallinity obtained thus have manifested that β -spherulites fall into Type IV and their lamellae exhibit a correlated and dendritic structure.

REFERENCES

1. P. M. McGenity, J. J. Hooper, C. D. Paynter, A. M. Riley, C. Nutbeem, N. J. Elton, and J. M. Adams, *Polymer*, **33**, 5215 (1992).
2. H. D. Keith, F. J. Padden, Jr., N. M. Walter, and H. W. Wyckoff, *J. Appl. Phys.*, **30**, 1485 (1959).
3. A. T. Jones, J. M. Aizlewood, and D. R. Beckett, *Makromol. Chem.*, **75**, 134 (1964).
4. J. Garbarczyk, *Makromol. Chem.*, **186**, 2145 (1985).
5. T. Yoshida, Y. Fujiwara, and T. Asano, *Polymer*, **24**, 925 (1983).
6. H. J. Leugering, *Makromol. Chem.*, **109**, 204 (1967).
7. J. Garbarczyk and D. Paukszta, *Polymer*, **22**, 562 (1981).
8. P. Jacoby, B. H. Bersted, W. J. Kissel, and C. E. Smith, *J. Polym. Sci. Part B Polym. Phys.*, **24**, 461 (1986).
9. G.-Y. Shi and J.-Y. Zhang, *Kexue Tongbao*, **27**, 290 (1982).
10. A. J. Lovinger, J. O. Chua, and C. C. Gryte, *J. Polym. Sci. Polym. Phys. Ed.*, **15**, 641 (1977).
11. H. Dragaun, H. Hubeny, and H. Muschik, *J. Polym. Sci. Polym. Phys. Ed.*, **15**, 1779 (1977).
12. M.-R. Huang, Master Thesis, China Textile University, Shanghai, China, 1987.
13. D. R. Norton and A. Keller, *Polymer*, **26**, 704 (1985).
14. G.-Y. Shi, B. Huang, J.-Y. Zhang, and Y.-H. Cao, *Sci. Sin. Ser. B*, **30**, 225 (1987).
15. R. Janarthanan, S. N. Garg, and A. Misra, *J. Appl. Polym. Sci.*, **51**, 1175 (1994).

Received June 21, 1994

Accepted October 15, 1994